



HAL
open science

Structure of the Mesophases Formed by a Perfluoroalkyl/Biphenyl Compound. Amphiphilic and Steric Effects

Sandrine Pensec, François-Genès Tournilhac, Pierre Bassoul

► **To cite this version:**

Sandrine Pensec, François-Genès Tournilhac, Pierre Bassoul. Structure of the Mesophases Formed by a Perfluoroalkyl/Biphenyl Compound. Amphiphilic and Steric Effects. *Journal de Physique II*, 1996, 6 (11), pp.1597-1605. 10.1051/jp2:1996150 . jpa-00248395

HAL Id: jpa-00248395

<https://hal.science/jpa-00248395>

Submitted on 4 Feb 2008

HAL is a multi-disciplinary open access archive for the deposit and dissemination of scientific research documents, whether they are published or not. The documents may come from teaching and research institutions in France or abroad, or from public or private research centers.

L'archive ouverte pluridisciplinaire **HAL**, est destinée au dépôt et à la diffusion de documents scientifiques de niveau recherche, publiés ou non, émanant des établissements d'enseignement et de recherche français ou étrangers, des laboratoires publics ou privés.

Structure of the Mesophases Formed by a Perfluoroalkyl/Biphenyl Compound. Amphiphilic and Steric Effects

Sandrine Pensec, François-Genès Tournilhac (*) and Pierre Bassoul

Chimie et Électrochimie des Matériaux Moléculaires (**), ESPCI, 10 rue Vauquelin,
75231 Paris Cedex 05, France

(Received 21 June 1996, received in final form 23 July 1996, accepted 31 July 1996)

PACS.61.30.Eb – Experimental determinations of smectic, nematic, cholesteric, and other structures

Abstract. — We describe the synthesis and mesomorphic behaviour of 4-(1H,1H-perfluoro-octyloxy)-4'-methoxy biphenyl. Two mesophases of smectic E and smectic A types were observed. X-ray diffraction study of the smectic E phase indicates a herringbone arrangement of the biphenyl cores, the perfluoroalkyl chains being in a molten state. The $S_E \rightarrow S_A$ transition is related to the melting of the biphenyl sublattice. In both phases, the flexibility of perfluoroalkyl chains permits the area matching between the two segregated sublayers.

Résumé. — Nous décrivons la synthèse et les propriétés mésomorphes du 4-(1H,1H-perfluoro-octyloxy)-4'-méthoxy biphenyle. Ce composé forme deux mésophases de type smectique E et smectique A. L'analyse par diffraction des rayons X révèle, dans le cas de la phase smectique E un arrangement en chevrons des cœurs biphenyles, les chaînes perfluoroalkyles se trouvant dans un état désordonné. La transition $S_E \rightarrow S_A$ correspond à la fusion partielle de la sous-couche biphenyle. Dans les deux phases smectiques, la flexibilité des chaînes perfluoroalkyles permet l'adéquation des aires moléculaires entre les deux sous-couches ségréguées.

1. Introduction

The macroscopic properties of molecular materials are closely related to the type of symmetry and organization existing in the condensed phase considered [1]. The amphiphilic character, which is commonly used for understanding the self assembling ability of lyotropic substances is now recognized to be relevant even for thermotropic mesophases [2]. In this latter case mesogens have a polarizable rigid core bearing one or several flexible side chains [3]. They can be considered as amphiphilic molecules as soon as the two different chemical fragments segregate in the smectic layers.

We describe the synthesis and X-ray study of a biphenyl substance made up of a biaryl core and a perfluoroalkyl chain. Due to the great polarizability difference [4] these two fragments are expected to display an enhanced amphiphilic character. Detailed structural information obtained from X-ray diffraction allows us to discuss the relationships between the characteristics of the molecule and the mesophase organization.

(*) Author for correspondence (e-mail: fgt@cis.espci.fr)

(**) URA 429 CNRS

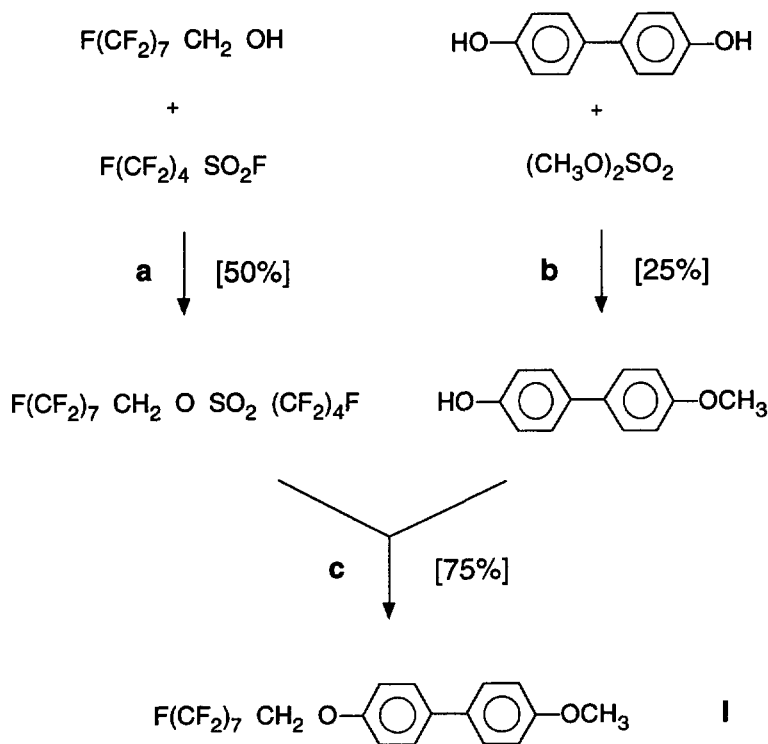


Fig. 1. — Synthetic pathway utilized for preparation of mesogen. **I**. (a): NEt_3 ; CH_2Cl_2 ; $-50\text{ }^\circ\text{C}$. (b): 10% (w/w) NaOH in water; RT (c): K_2CO_3 ; DMF ; $90\text{ }^\circ\text{C}$.

2. Synthesis

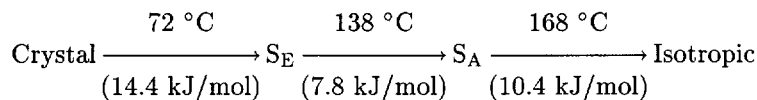
The synthetic scheme is depicted in Figure 1. 4,4' dihydroxydiphenyl (Fluka) was alkylated with dimethyl sulphate in the conditions required for precipitation of the monomethyl ether [5], (Yield: 25%) whereas 1H,1H-perfluorooctanol was activated with the aid of perfluorobutane-sulphonyl fluoride [6] (50%). Both compounds were then reacted in standard conditions to give the 4-methoxy, 4-(1H,1H- perfluorooctyloxy) diphenyl **I** with a 75 percent yield. The purity was checked at each step by NMR, infrared spectroscopy and mass spectrometry. Owing to its insolubility, the final compound was purified by liquid chromatography at $60\text{ }^\circ\text{C}$ followed by recrystallization.

3. Mesomorphic Behaviour

Optical microscopy was carried out using a Leitz Orthoplan polarizing microscope equipped with a Mettler FP52 hot stage. On heating, melting of the crystalline phase was observed at $72\text{ }^\circ\text{C}$, followed by a broad mesomorphic domain ($72 - 170\text{ }^\circ\text{C}$). On cooling ($-5\text{ }^\circ\text{C}/\text{min}$) from the isotropic phase, the birefringence was detected at $170\text{ }^\circ\text{C}$ by appearance of focal conics domains [7]. The mesophase was identified as smectic A (S_A) since the homeotropic texture was also observed in the same temperature range. At $138.5\text{ }^\circ\text{C}$, the focal conics fans become crossed with concentric lines and at the same temperature, a greyish coloration appears in

homeotropic domains. These textures are characteristic of the smectic E phase (S_E) [7]. Then, the S_E phase was overcooled down to room temperature.

DSC thermograms were recorded at ± 5 °C per minute using a Perkin-Elmer DSC 7 apparatus. Temperatures and enthalpies measured for the phase transitions are the following:



Transitions between different crystalline phases detected below 70 °C will not be discussed in this paper.

4. X-Ray Study of the Mesophases

4.1. EXPERIMENTAL. — Due to the biaxial symmetry, smectic E single domains cannot be formed simply from smectic A oriented samples. In order to obtain quantitative measures of X-ray intensities, we decided to investigate powder samples. The compounds were analysed using three different X-ray diffraction methods. In all cases, the $\text{CuK}\alpha$ radiation was used. Accurate measures of diffraction angles were obtained using a Guinier type camera (Tab. I). This method permitted to separate $hk0$ and hkl reflections arising at very close angles. The presence of hkl reflections was confirmed by recording diffraction profiles with a Rigaku PMG-S2 $\theta - 2\theta$ goniometer stage equipped with a thermally controlled sample holder (Fig. 2c). Relative intensities of $00l$ reflections were estimated by scanning the films obtained with a Debye-Scherrer chamber (Figs. 2a, 2b, Tab. II).

4.2. RESULTS. — Diffraction diagrams of the smectic E phase were recorded at 101 °C (Tab. I). They contain five $00l$ sharp reflections at small angles corresponding to an interlayer distance of $c = 28.8$ Å. At larger angles five $hk0$ reflections were indexed with a 2D rectangular unit cell of parameters $a = 8.0$ Å and $b = 5.6$ Å. The presence of a 111 peak near the 110 one (Fig. 2c) indicates that a 3D orthorhombic cell should be taken to describe the structure of this smectic phase. In all experiments, a broad scattering signal with a maximum at $q = 1.15$ Å⁻¹ was recorded (Fig. 2a) hence indicating that a liquid like order with an average molecular distance of $r = \frac{2}{\sqrt{3}} \frac{2\pi}{q} = 6.3$ Å⁽¹⁾ is also present within the layers.

The diffraction pattern of the smectic A phase was recorded at 150 °C (Fig. 2b). The layered structure is now evidenced by the presence of three $00l$ sharp reflections corresponding to an interlayer distance of 28.4 Å. At wide angles, the diffuse scattering profile which is characteristic of the smectic A phase can be decomposed into two Gaussian peaks centered at $q = 1.08$ and $q = 1.31$ Å⁻¹. The corresponding distances $r_1 = 6.8$ Å and $r_2 = 5.5$ Å⁽¹⁾ are therefore necessary to describe the liquid like order existing in this phase.

5. Structure of the Smectic E Layers

5.1. STERIC ANALYSIS OF THE MOLECULAR PACKING. — In the smectic E phase, the unit cell is a parallelepiped of dimensions $a = 8.0$ Å, $b = 5.6$ Å, $c = 28.8$ Å. The molecular length given by CPK models in the fully extended conformation is of about 23.3 Å which is significantly smaller than the interlayer distance. A bimolecular packing should therefore be postulated. With two molecules per unit cell, the calculated density is 1.45 which is a quite

(¹) For estimation of these distances, we consider that the local order is close to an hexagonal packing.

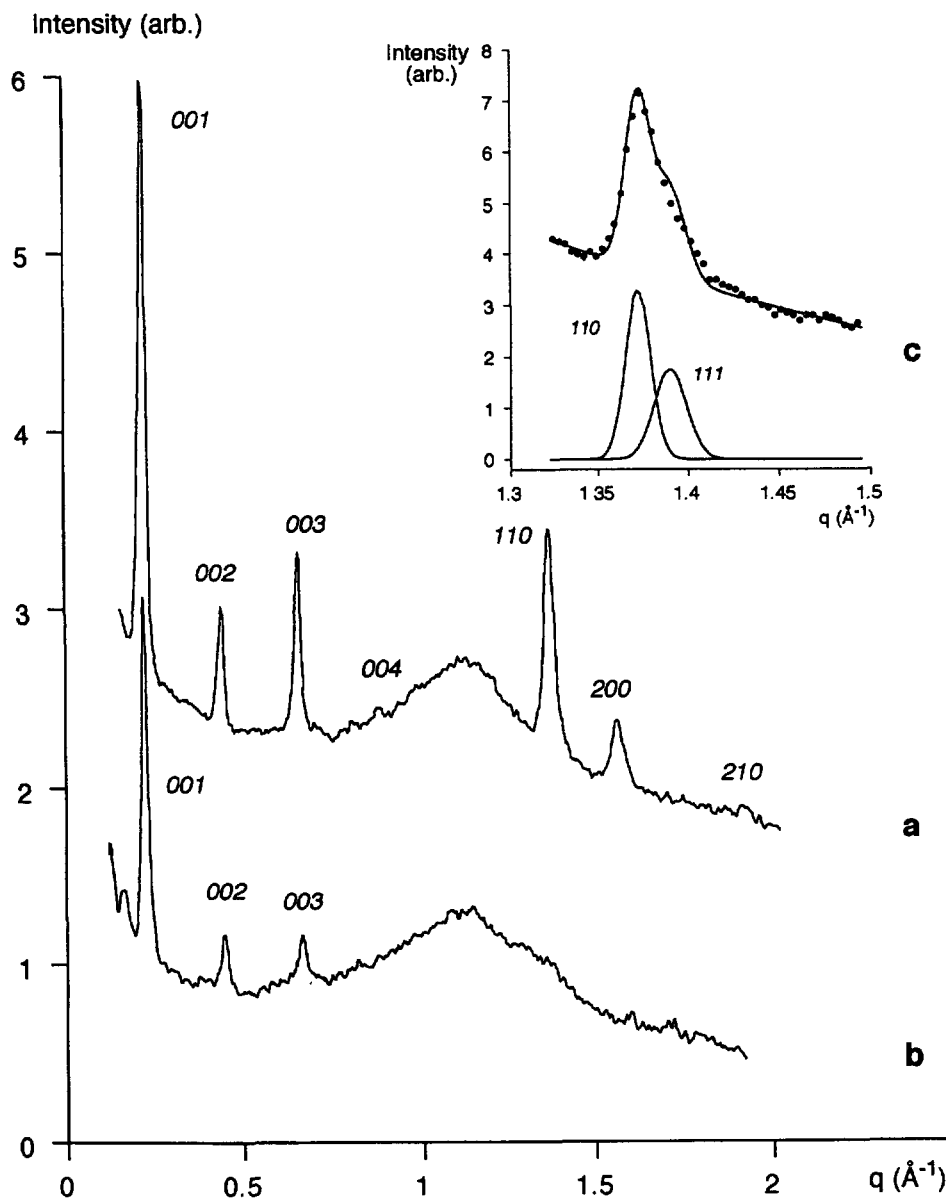


Fig. 2. — X-ray diffraction profiles of compound I as a function of $q = 2\pi/d_{hkl}$ obtained from microdensitometry of Debye-Scherrer films, for the smectic E phase (a) and for the smectic A phase (b). The inset (c) shows the overlap of the 110 and 111 reflections: the dotted line represents the experimental points recorded with a goniometer stage, decomposition into two Gaussian peaks is shown below.

realistic value for highly fluorinated compounds [8]. We will therefore consider the various bimolecular packings which are compatible with the rectangular in-plane order.

The area available per unit cell in the plane of the layers is $a \cdot b = 44.8 \text{ \AA}^2$. A first model (Fig. 3a)

Table I. — d_{hkl} calc. are calculated from an orthorhombic cell of parameters $a = 8.0$, $b = 5.6$, $c = 28.8$ Å. d_{hkl} exp. have been measured using a Guinier camera (a) or a goniometer stage (b).

d_{hkl} exp. (Å)	d_{hkl} calc. (Å)	hkl
28.78 (a)	28.82	001
14.40 (a)	14.41	002
9.62 (a)	9.60	003
7.21 (a)	7.20	004
-	5.76	005
4.80 (b)	4.80	006
5.45 (a)	-	halo
4.58 (b)	4.58	110
4.52 (b)	4.52	111
4.01 (a)	4.01	200
3.26 (a)	3.26	210
2.65 (a)	2.64	120
2.42 (a)	2.41	310

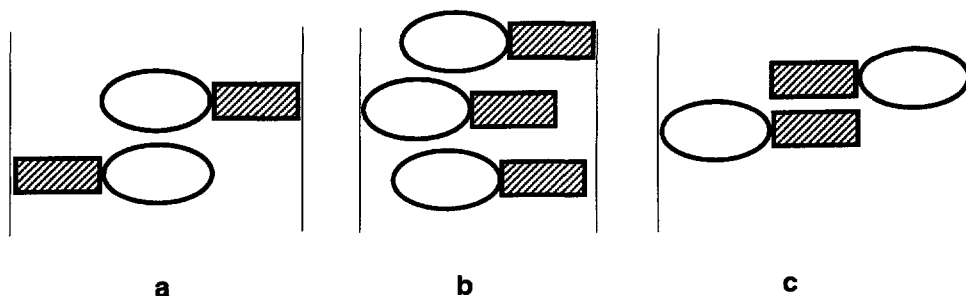


Fig. 3. — The three hypothetical types of packing. (a) with overlap of the chains (b) with polar symmetry (c) with overlap of the cores.

with overlapped perfluoroalkyl chains can be assumed. In the crystalline phase, perfluoroalkyl chains have a cross section of 28 \AA^2 [9]. Two perfluoroalkyl chains in the mesomorphic state should occupy an area larger than 56 \AA^2 . The second model (Fig. 3b) with a polar symmetry should be excluded for the same reason. Then the only remaining possibility is to overlap the two biphenyl cores (Fig. 3c).

The cross section of two biphenyl cores calculated from crystal data [10] is 44 \AA^2 . This value perfectly fits the space available. In the model of Figure 3c, the two molecules in their

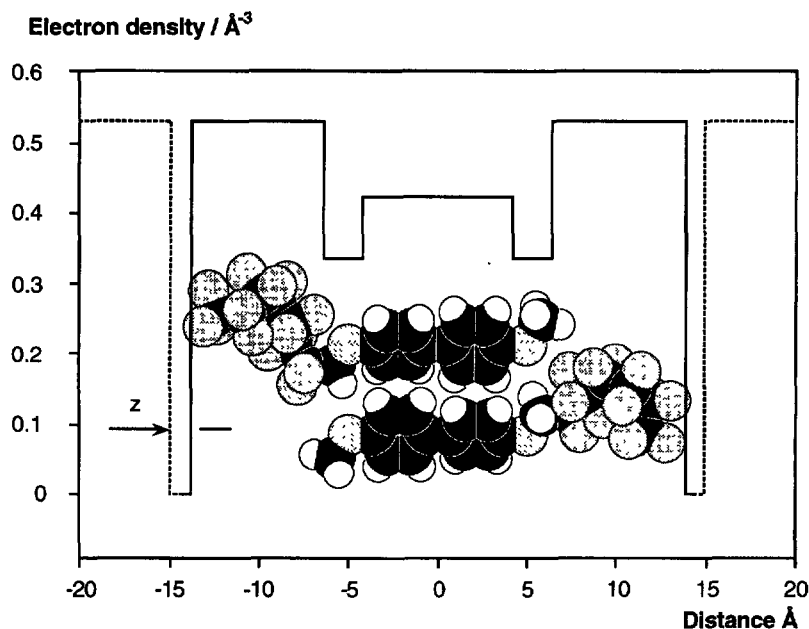


Fig. 4. — Model for the repartition of molecular cores and chains in the smectic E layer. The corresponding mean electron density profile perpendicular to the layers taken to calculate the X-ray intensities is shown.

fully extended conformation would lead to an interlayer distance of 34 \AA which is greater than observed. On the other hand, in order to fill the 44.8 \AA^2 available, each perfluoroalkyl chain has to take a disordered conformation consistent with the presence of a halo in the diffraction figure. According to this model, the biphenyl units and their oxymethylene groups are overlapped by a length of about 12.8 \AA . Hence the space available for each perfluoroalkyl chain is of 358 \AA^3 . By considering the molar volume of perfluoroalkanes in the liquid state [11], we calculated a molecular volume of 320 \AA^3 for the C_7F_{15} fragment. Perfluoroalkyl chains in a liquid like conformation may optimize the packing. Such an arrangement is schematically represented in Figure 4.

In smectic E phases formed by non fluorinated mesogens [12], a rectangular 2D cell has been taken to describe the herringbone packing of biphenyls. In the present case, four different space groups are compatible with the reflections observed: $P22_12$, $Pma2$, $Pba2$ and $P2_12_12$. The former group does not generate a compact packing of the phenyl cores; $Pma2$ and $Pba2$ cannot give perfluoroalkyl chains in opposite directions (Fig. 3c); then the only possibility is $P2_12_12$. In Figure 5, we have represented the packing of the biphenyl units related by the symmetry elements of this space group. The electron density profile taken from the model of Figure 4 is satisfactory to explain the relative intensities of the $00l$ reflections (Tab. II).

5.2. X-RAY INTENSITIES ANALYSIS. — The intensities of the layer period harmonics $I(q_{00l})$ are collected in Table II.

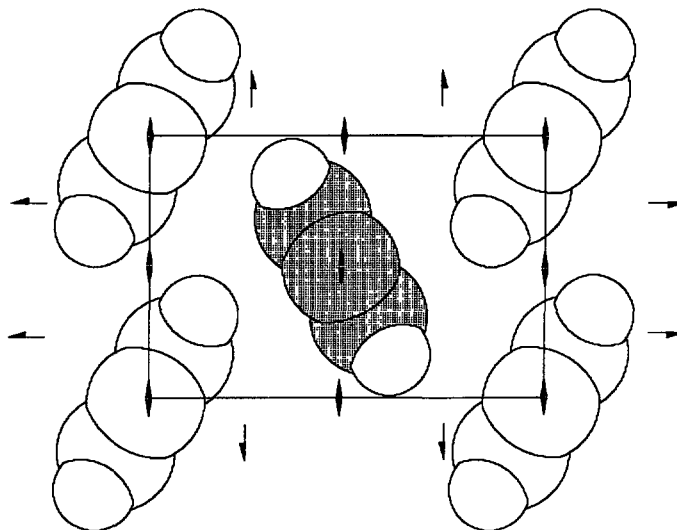


Fig. 5. — Herringbone packing of biaryl cores. The symmetry elements of the $P2_12_12$ group are shown. Light and dark molecules have perfluoroalkyl chains pointing up and down respectively.

Table II. — *Experimental values of intensities of the 00l reflections in the S_E and S_A phases and calculated values from the model of Figure 4.*

	<i>hkl</i>	001	002	003	004
Smectic E	exp.	100	18	27	2
	calc.	100	17	30	1
Smectic A	exp.	100	14	12	-
	calc.	100	13	13	0.2

Surprisingly, the third harmonic is stronger than the second one in the smectic E phase. For powder diffraction patterns of a crystal, the intensity of a 00l reflection is given by [13]:

$$I(q_{00l}) \propto \frac{1}{q_{00l}^2} |F(q_{00l})|^2 \exp(-\sigma^2 q_{00l}^2) \quad (1)$$

$1/q_{00l}^2$ is the relevant Lorentz correction factor for the Debye-Scherrer experiment, $F(q_{00l})$ is the structure factor and σ the Debye-Waller coefficient. For liquid crystals, similar expressions have been established [14] which consider the diffraction by infinitely thin surfaces. In this approximation, $|F(q_{00l})|^2$ is equal to unity. This approach cannot explain the nonmonotonic decay of the intensities $I(q_{00l})$ observed in our case. Molecular form factor of related fluorinated materials have been calculated by several authors [15,16]. We have utilized the electron density profile of Figure 4 to calculate the intensities of the 00l reflections. In our model, the different molecular fragments are characterized by their electronic densities. Formula (1) was applied using two adjustable parameters: z , the width of the interlayer gap (Fig. 4) and σ , the Debye-Waller coefficient. The results of the best fit are collected in Table II, the values of $z = 1.1 \text{ \AA}$ and $\sigma = 1.3 \text{ \AA}$ were found. These two values of the order of one interatomic distance

give an estimate of the layer roughness. The above analysis confirms the picture of well segregated sublayers with limited motions of the molecules across the layers.

6. Smectic A Phase

At the transition from smectic E to smectic A phases, the herringbone packing of biphenyls disappears. The transition enthalpy is very close to the one reported for nonfluorinated mesogens [7]. This suggests that the melting of the aromatic sublattice is the principal feature of this transformation. The double halo which is observed in the smectic A is now related to two different intralayer distances: i) the mean core-to-core distance of biphenyl units (5.5 Å) and ii) the interchain distance of 6.7 Å already found in the smectic E phase. This indicates that the two antagonistic parts of the molecule are located in two distinct sublayers even though both are in a quasi-molten state. As previously mentioned for smectic A phases formed by polyphilic molecules [17], the double halo which is observed in the wide angle region can be regarded as the signature of the segregated arrangement. In the smectic E phase, each core has two neighbours at a distance of 5.6 Å and four at 4.9 Å. The mean intermolecular distance estimated in the smectic A phase (5.5 Å) is intermediate between these two figures. It is therefore reasonable to propose that the local order existing in the biphenyl sublattice is close to the herringbone packing but with short-range correlations.

As previously mentioned for other polyfluorinated mesogens [16], the ratio of intensity of the second harmonic to the first is two orders of magnitude higher than in conventional smectic A materials. This fact can be correlated with the enhanced amphiphilic character of semi-perfluorinated compounds. The electron density profile defined for the smectic E phase is still valid for fitting the intensities of the $00l$ reflections in the smectic A (Tab. II). The best fit was obtained with $z = 1.1$ Å and $\sigma = 2.0$ Å; the latter value, whilst being higher than in smectic E again indicates the sharpness of interfacial regions.

The interlayer distance was found to decrease slightly when entering the smectic A phase. This can be rationalized by considering that perfluoroalkyl chains have to take a more disordered conformation to match the higher cross section of biphenyl rings.

7. Conclusion

The formation of segregated sublayers containing two antagonistic parts of the molecule has been evidenced from X-ray diffraction analysis. In the smectic E phase, the dimensions of the rectangular cell are almost identical to those reported for nonfluorinated mesogens [12] meaning that the herringbone packing of these moieties is not altered by the nature of the flexible chains.

In comparison to previous investigations of nonfluorinated smectic E materials, the present study reveals the coexistence of liquid like perfluoroalkyl chains with well crystallized biphenyl sublayers. This was not really expected since perfluoroalkyl chains are stiffer than alkyl ones. In the present case, the area matching between the two sublayers determines the perfluoroalkyl chain conformation.

Acknowledgments

It is a pleasure to thank D. Lelièvre for X-ray measurements, and A.M. Levelut for help in using the Guinier camera and for discussion.

References

- [1] Simon J., Bassoul P. and Norvez S., *New. J. Chem.* **13** (1989) 13.
- [2] Skoulios A. and Guillon D., *Mol. Cryst. Liq. Cryst.* **165** (1988) 317.
- [3] Demus D. and Zschke H., *Flüssige Kristalle in Tabellen II* (VEB Verlag, Leipzig, 1984).
- [4] Barton A.F.M., *Handbook of Solubility Parameters*, 2nd ed. (CRC Press, Boca Raton, 1991).
- [5] Alphen J.V., *Rec. Trav. Chim.* (The Netherlands) **50** (1931) 657.
- [6] Hansen R.L., U.S. Patent (1968) 3,419,595.
- [7] Gray G.W. and Goodby J.W.G., *Smectic Liquid Crystals* (Leonard Hill, Glasgow, 1984).
- [8] Kromm P., Thesis, Bordeaux (1996).
- [9] Klark E.S. and Muus L.T., *Z. Krist.* **117** (1962) 119.
- [10] Schudt E. and Weitz G., Structure data of organic crystals in Landolt-Börnstein, Zahlenwerte und Funktionen aus Naturwissenschaft und Technik, vol. III/5a, p. 645, vol. III/5b, pp. 909, 1100, 1193, 1243 (Springer Verlag, Berlin, 1971).
- [11] Hudlicky M., *Chemistry of Organic Fluorine Compounds*, 2nd ed. (Ellis Horwood, Chichester, 1976).
- [12] Doucet J., Levelut A.M., Lambert M., Liébert L. and Strzelecki L., *J. Phys. Colloq. France* **36** (1975) C1-13.
- [13] Guinier A., *Théorie et technique de la radiocristallographie*, 2nd ed. (Dunod, Paris, 1956).
- [14] Caillé A., *C. R. Acad. Sci. Paris, B* **274** (1972) 891.
- [15] Rabolt J.F., Russel T.P. and Twieg R.J., *Macromolecules* **17** (1984) 2786.
- [16] Lobko T.A., Ostrovskii B.I., Pavluchenko A.I. and Sulianov S.N., *Liq. Cryst.* **15** (1993) 361.
- [17] Blinov L.M., Lobko T.A., Ostrovskii B.I., Sulianov S.N. and Tournilhac F.G., *J. Phys. II France* **3** (1993) 1121.